Agricultural and Forest Meteorology 152 (2012) 212–222

Contents lists available at SciVerse ScienceDirect

Agricultural and Forest Meteorology

journal homepage: www.elsevier.com/locate/agrformet

On the temporal upscaling of evapotranspiration from instantaneous remote sensing measurements to 8-day mean daily-sums

Youngryel Ryu[a,s,*], Dennis D. Baldocchi[a], T. Andrew Black[b], Matteo Detto[c], Beverly E. Law[d], Ray Leuning[e], Akira Miyata[f], Markus Reichstein[g], Rodrigo Vargas[h], Christof Ammann[i], Jason Beringer[j], Lawrence B. Flanagan[k], Lianhong Gu[l], Lindsay B. Hutley[m], Joon Kim[n], Harry McCaughey[o], Eddy J. Moors[p], Serge Rambal[q], Timo Vesala[r]

[a] Dep. of Environmental Science, Policy and Management, University of California, Berkeley, CA, USA
[b] Faculty of Land and Food Systems, University of British Columbia, British Columbia, Canada
[c] Smithsonian Tropical Research Institute, Panama
[d] Dep. of Forest Ecosystems and Society, Oregon State University, Corvallis, OR, USA
[e] CSIRO Marine and Atmospheric Research, Canberra, Australia
[f] National Institute for Agro-Environmental Sciences, Tsukuba, Japan
[g] Max-Planck Institute for Biogeochemistry, Jena, Germany
[h] Departamento de Biología de la Conservación, Centro de Investigación Científica y de Educación Superior de Ensenada (CICESE), BC, Mexico
[i] Agroscope ART, Federal Research Station, Zürich, Switzerland
[j] School of Geography and Environmental Science, Monash University, Victoria, Australia
[k] Dep. of Biological Sciences, University of Lethbridge, Lethbridge, Alberta, Canada
[l] Environmental Sciences Division, Oak Ridge National Laboratory, TN, USA
[m] Research Institute for the Environment and Livelihoods, Charles Darwin University, Darwin, Australia
[n] Dep. of Landscape Architecture and Rural System Engineering, Seoul National University, Seoul, South Korea
[o] Dep. of Geography, Queen's University, Kingston, Ontario, Canada
[p] ESS-CC, Alterra – Wageningen UR, Wageningen, The Netherlands
[q] DREAM, CEFE-CNRS, Montpellier, France
[r] University of Helsinki, Dept. of Physics, Helsinki, Finland
[s] Dep. of Organismic and Evolutionary Biology, Harvard University, Cambridge, MA, USA

ARTICLE INFO

Article history:
Received 3 December 2010
Received in revised form 23 August 2011
Accepted 12 September 2011

Keywords:
Evapotranspiration
Eddy covariance
Temporal upscaling
FLUXNET
MODIS

ABSTRACT

The regular monitoring of evapotranspiration from satellites has been limited because of discontinuous temporal coverage, resulting in snapshots at a particular point in space and time. We developed a temporal upscaling scheme using satellite-derived instantaneous estimates of evapotranspiration to produce a daily-sum evapotranspiration averaged over an 8-day interval. We tested this scheme against measured evapotranspiration data from 34 eddy covariance flux towers covering seven plant functional types from boreal to tropical climatic zones. We found that the ratio of a half-hourly-sum of potential solar radiation (extraterrestrial solar irradiance on a plane parallel to the Earth's surface) between 10:00 hh and 14:00 hh to a daily-sum of potential solar radiation provides a robust scaling factor to convert a half-hourly measured evapotranspiration to an estimate of a daily-sum; the estimated and measured daily sum evapotranspiration showed strong linear relation ($r^2 = 0.92$) and small bias (−2.7%). By comparison, assuming a constant evaporative fraction (the ratio of evapotranspiration to available energy) during the daytime, although commonly used for temporal upscaling, caused 13% underestimation of evapotranspiration on an annual scale. The proposed temporal upscaling scheme requires only latitude, longitude and time as input. Thus it will be useful for developing continuous evapotranspiration estimates in space and time, which will improve continuous monitoring of hydrological cycle from local to global scales.

1. Introduction

Evapotranspiration (E) is a major component of the terrestrial hydrological cycle (ca. 60% of land precipitation) (Trenberth et al., 2007). It controls land-atmosphere feedbacks via modulating land

* Corresponding author at: Department of Landscape Architecture and Rural Systems Engineering, Seoul National University, Seoul 151-921, South Korea. Tel.: +82 2 880 4871; fax: +82 2 873 5113.
E-mail address: yryu@snu.ac.kr (Y. Ryu).

0168-1923/$ – see front matter © 2011 Elsevier B.V. All rights reserved.
doi:10.1016/j.agrformet.2011.09.010

Table 1
Site information. CRO: crop, DBF: deciduous broadleaved forest, EBF: evergreen broadleaved forest, ENF: evergreen needle leaved forest. GRA: grassland, MF: mixed forest, WSA: woody savanna.[a]

PFT	Site ID	Country and site names	Lat	Lon	Year	Climate	References
CRO	US-Bo1	US – Bondville	40.0	−88.3	1998	Temperate	Meyers and Hollinger (2004)
	DE-Geb	Germany – Gebesee	51.1	10.9	2004	Temperate	Anthoni et al. (2004)
	JP-Mas	Japan – Mase paddy flux site	36.1	140.0	2002	Temperate	Saito et al. (2005)
	KR-Hnm	Korea – Haenam	34.6	126.6	2006	Temperate	Ryu et al. (2008b)
	US-Ne1	US – NE Mead	41.2	−96.5	2004	Temperate	Verma et al. (2005)
DBF	CA-Oas	Canada – SSA old aspen	53.6	−106.2	2004	Boreal	Krishnan et al. (2006)
	DE-Hai	Germany – Hainich	51.1	10.5	2004	Temperate	Kutsch et al. (2008)
	US-MOz	US – Missouri Ozark Site	38.7	−92.2	2005	Sub-tropical, Mediterranean	Gu et al. (2007)
	US-Bar	US – Bartlett	44.1	−71.3	2005	Temperate	Richardson et al. (2007)
	IT-Ro1	Italy – Roccarespampani 1	42.4	11.9	2004	Sub-tropical, Mediterranean	Tedeschi et al. (2006)
	IT-Ro2	Italy – Roccarespampani 2	42.4	11.9	2004	Sub-tropical, Mediterranean	Tedeschi et al. (2006)
EBF	FR-Pue	France – Puechabon	43.7	3.6	2006	Sub-tropical, Mediterranean	Allard et al. (2008)
	IT-Cpz	Italy – Castelporziano	41.7	12.4	2004	Sub-tropical, Mediterranean	Reichstein et al. (2007)
	AU-Tum	Australia – Tumbarumba	−35.7	148.2	2003	Temperate	Leuning et al. (2005)
	ID-Pag	Indonesia – Palangkaraya	2.3	114.0	2002	Tropical	Hirano et al. (2007)
ENF	FI-Hyy	Finland – Hyytiälä	61.8	24.3	2006	Boreal	Suni et al. (2003)
	KR-Kw2	Korea – Kwangneung2	37.7	127.1	2008	Temperate	Hong et al. (2008)
	NL-Loo	Netherlands – Loobos	52.2	5.7	2006	Temperate	Dolman et al. (2002)
	US-Blo	US – Blodgett Forest	38.9	−120.6	2002	Subtropical	Goldstein et al. (2000)
	US-Me2	US – Metolius2	44.5	−121.6	2004	Sub-tropical, Mediterranean	Thomas et al. (2009)
	US-Me3	US – Metolius3	44.3	−121.6	2004	Sub-tropical, Mediterranean	Vickers et al. (2010)
GRA	CH-Oe1	Switzerland – Oensingen1 grass	47.3	7.7	2006	Temperate	Ammann et al. (2007)
	NL-Ca1	Netherlands – Cabauw	52.0	4.9	2006	Temperate	Jacobs et al. (2007)
	US-Var	US – Vaira ranch	38.4	−121.0	2006	Sub-tropical, Mediterranean	Ryu et al. (2008a)
	CA-Let	Canada – Lethbridge	49.7	−112.9	2005	Temperate	Flanagan et al. (2002)
	DE-Meh	Germany – Mehrstedt	51.3	10.7	2005	Temperate	Scherer-Lorenzen et al. (2007)
	US-Snd	US – Sherman Island	38.0	−121.8	2008	Sub-tropical, Mediterranean	Detto et al. (2010)
MF	BE-Vie	Belgium – Vielsalm	50.3	6.0	2002	Temperate	Aubinet et al. (2001)
	CA-Gro	Canada – Groundhog River	48.2	−82.2	2005	Boreal	McCaughey et al. (2006)
	CA-WP1	Canada – Western Peatland	55.0	−112.5	2005	Boreal	Syed et al. (2006)
WSA	US-SRM	US – Santa Rita Mesquite	31.8	−110.9	2005	Dry	Scott et al. (2009)
	US-SO2	US – Sky Oaks-Old Stand	33.3	−116.6	2006	Sub-tropical, Mediterranean	Luo et al. (2007)
	AU-How	Australia – Howard Springs	−12.5	131.2	2003	Tropical	Beringer et al. (2007)
	US-Ton	US – Tonzi ranch	38.4	−121.0	2005	Sub-tropical, Mediterranean	Baldocchi et al. (2004)

[a] The classification and definition of PFT followed IGBP convention (Loveland et al., 2000).

surface energy budget, and constitutes an important source of water vapor to the atmosphere (Raupach, 1998). In turn, atmospheric water vapor is the most significant greenhouse gas and thus plays a fundamental role in weather and climate (Held and Soden, 2000; IPCC, 2007). Understanding E is important for socio-economic reasons, such as regulating available water for human use (Brauman et al., 2007). Thus, there have been diverse efforts to monitor E regularly in a regional scale using satellite remote sensing imagery (Anderson et al., 2008; Diak et al., 2004; Nishida et al., 2003).

The applicability of remote sensing-based estimates of E is hampered because satellites have limited temporal coverage, resulting in snapshots of E at a particular point in space and time. Thus, it is a challenge to compare E estimates from different sites that are taken at different times of the day. For practical purposes, time-integrated E is more meaningful for managing water resources and for comparison with accumulated precipitation (Baldocchi and Ryu, 2011). An 8-day mean daily sum is selected in this study as the 8-day period corresponds to the cycle of MODIS global coverage (Masuoka et al., 1998).

A common approach to estimate time-integrated E is to assume that the evaporative fraction, EF, (the ratio of latent heat flux, λE, to available energy, A, which is taken to be equal to the net radiation (R_n) minus the soil heat flux (G)) is constant during daytime, so daytime total E can be estimated by multiplying an instantaneous EF and daytime integrated A (Brutsaert and Sugita, 1992; Crago, 1996; Jackson et al., 1983; Verma et al., 1992). Anderson et al. (2007) further developed this idea by coupling a planetary boundary layer model with two snapshots in the morning from Geostationary Operational Environmental Satellites (GOES) for calculating instantaneous λE and EF, and finally extrapolated these values to a daily scale using hourly A derived from GOES. However, the constant EF assumption was developed in homogeneous grasslands or crops. In addition, one study reported that EF varies considerably during daytime depending on soil moisture status and leaf area index (Leuning et al., 2004). Satellite-based estimation of instantaneous soil heat flux is still a challenge, in particular for open canopies. In fact, the constant EF approach was identified as a major source of uncertainty in the remote sensing-based E estimates (Ferguson et al., 2010).

An alternative approach includes developing a constant linear regression equation between mid-day flux values and the daily mean flux values using flux tower data. For example, Sims et al. (2005) tested a linear regression between a single-hour extraction of gross primary productivity (GPP) to a mean value of 24-h GPP for a 8-day period using flux tower data. These authors found a consistent linear regression that held across a range of plant functional types and times of year, based on 8 eddy covariance flux towers within the United States and Canada. However, it is unclear if the constant scaling factor holds in other latitudes and longitudes or if the technique is valid for E.

We report that both the constant EF and the constant scaling factor approaches do not provide robust upscaled estimates. Thus, developing an alternative scheme is warranted. We demonstrate that the averaged ratio of a half-hourly-sum of potential solar radiation (R_{gPOT}, extraterrestrial irradiance on a plane parallel to the

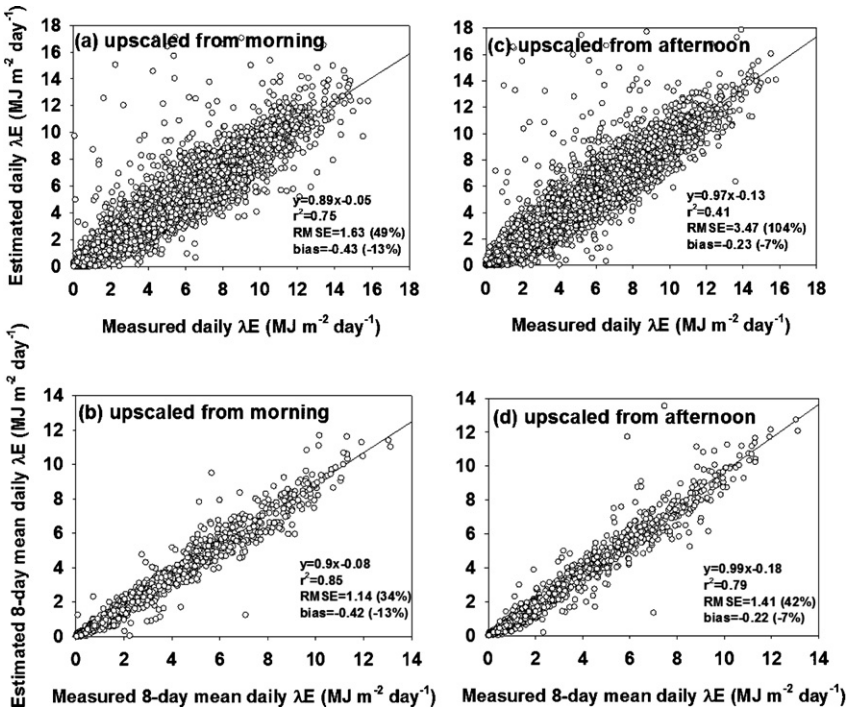

Fig. 1. Test of constant *EF* (the ratio of λE to available energy) approach using the 34 flux tower data. (a) Comparison between upscaled daily λE from a randomly selected half-hourly λE in the morning (10:00–12:00 hh) using the constant *EF* approach and measured daily λE. (b) Same with (a) except for 8-day mean daily scale. (c) Same with (a) except for selecting afternoon (12:00–14:00 hh). (d) Same with (c) except for using 8-day mean daily scale.

Earth's surface) to the daily-sum of R_{gPOT} over a 8-day period can be used to upscale instantaneous $\lambda E(t)$ to a 8-day mean daily sum λE. To test the efficacy of the scheme, we used data from 34 eddy covariance flux tower across 7 plant functional types spanning the range from boreal to tropical climatic zones. The scientific questions for this study include: (1) How does the upscaling factor from this new scheme vary with plant functional types and climatic zones?, (2) Can the upscaling scheme developed from the half-hourly flux tower data be used for instantaneous satellite data? and (3) Can the upscaling scheme be applied for estimation of other biological and environmental variables such as gross primary productivity (GPP) and solar irradiance?

2. Methods

2.1. Flux tower sites description and data processing

We analyzed λE data from 34 sites including 7 plant functional types (PFTs) ranging from boreal to tropical climatic zones extracted from LaThuile 2007 FLUXNET dataset v.2 (www.fluxdata.org) (Table 1). We selected at least three sites for each PFT which showed data gaps less than 30 days per year, and selected one year of measurements per site that was represented by a minimum data gaps over the available years. Data gaps were filled using the marginal distribution sampling method in an harmonized and standardized way for the LaThuile 2007 FLUXNET dataset (Reichstein et al., 2005). Mid-day half-hourly sums (e.g. 10:00–10:30 hh, 10:30–11:00 hh, . . ., 13:30–14:00 hh) of λE from flux towers were calculated to find a correspondence with potential overpass times of the MODIS Terra and Aqua satellites. Overpass times vary among and within sites because of changing sensor view angle and orbital mode of the satellites (i.e., ascending or descending) (Masuoka et al., 1998). The ratio of the half-hourly sums to the daily sums λE was averaged over 8-day periods that correspond to the cycle of MODIS global coverage (Masuoka et al., 1998).

2.2. MODIS-derived evapotranspiration model

Here we briefly introduce a novel MODIS derived λE model (Ryu et al., 2011), developed using a two-leaf (sunlit-shade) and a dual-source (vegetation and soil) λE model. The model first calculated instantaneous radiation components under all sky condition at 1 km resolution including incoming shortwave, direct beam photosynthetically active radiation (PAR) and diffuse PAR (Iwabuchi, 2006; Kobayashi and Iwabuchi, 2008), incoming longwave (Prata, 1996), outgoing longwave (Wan, 2008) and outgoing shortwave radiation (Schaaf et al., 2002). Those components enabled us to calculate instantaneous R_n over all sky conditions. For the closed canopy in temperate and boreal forests, we used MODIS albedo to estimate leaf nitrogen content, N(%) (Ollinger et al., 2008), which was converted to N (area based) via leaf mass per area based on a global dataset of leaf traits (Wright et al., 2004). Then maximum carboxylation rate at 25 °C (Vcmax) was quantified using the nitrogen use efficiency (i.e., Vcmax/N (area based)) (Kattge et al., 2009). For the other canopies, we used a look up table that classifies Vcmax with plant functional types and climate zones. The absorbed PAR calculated with PAR, LAI and clumping index (Pisek et al., 2010; Ryu et al., 2010a, 2010b) and Vcmax information allowed us to apply the Farquhar's photosynthesis model to the sun and shade leaves separately (dePury and Farquhar, 1997). We iteratively solved the sun and shade photosynthesis and energy balance equations until convergence of temperature in sun and shade leaves. The Ball-Berry equation calculated two-leaf canopy conductance (Collatz et al., 1991), which enabled us to couple photosynthesis and transpiration. To calculate canopy *E*, we applied a quadratic form of the Penman–Monteith equation separately for the sun and shade leaves (Paw U and Gao,

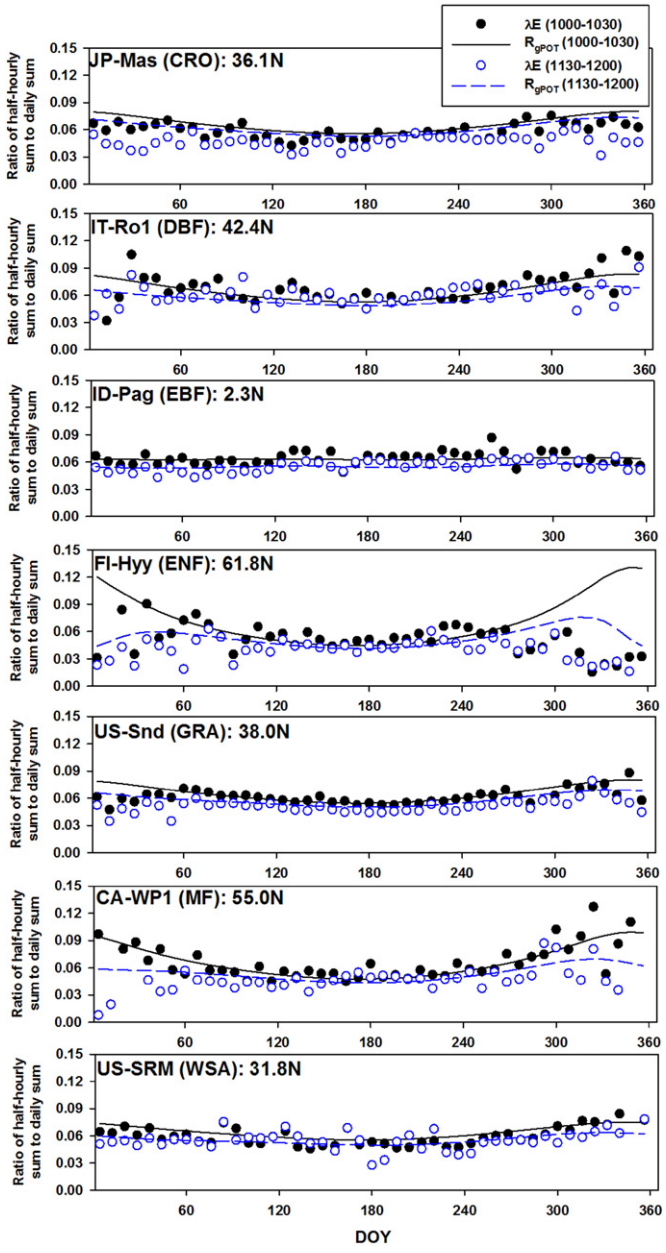

Fig. 2. Seasonal pattern of the ratios of half-hourly sum to the daily sum for latent heat flux (λE) and potential solar radiation (R_{gPOT}) using flux tower data. The ratios were averaged over an 8-day interval. Two half-hourly intervals (10:00–10:30 hh, 11:30–12:00 hh) were selected (see Section 2 for details).

1988). The soil E was calculated as the equilibrium E constrained by a water stress factor (RH^{VPD}) (Fisher et al., 2008). The modeled E was an instantaneous value under all sky condition as the main drivers (e.g. radiation components) were derived from MODIS snap-shots.

2.3. Development of temporal upscaling of evapotranspiration scheme

We hypothesized that the mean of diurnal variation of E over an 8-day interval scales with the respective mean diurnal variation of R_{gPOT} over the same interval. Several justifications include: (1) R_g is the main driver that controls E at the diurnal scale if there is no substantial asymmetry of cloudiness or change in soil moisture between morning and afternoon. Under clear or thick cloudy condition, R_{gPOT} scales with R_g. (2) the R_{gPOT} sets the daytime when most E happens. The daily cycles of R_{gPOT} and E are almost in phase. (3) The random variability in the diurnal variation of E is likely to be removed largely by averaging over an 8-day interval.

Table 2
Comparison between $R_{gPOT.0.5\,h}/R_{gPOT.day}$ and $\lambda E_{0.5\,h}/\lambda E_{day}$ averaged for morning (10:00–12:00 hh) and afternoon (12:00–14:00 hh) during the growing season. The growing season was defined between DOY 120 and 240 except for ID-Pag (DOY 1–365), US-Var (DOY 30–150), AU-Tum (DOY 1–60, 305–365). RMSE is root mean square error, bias is that the ratio of R_{gPOT} minus the ratio of λE. Typical values of the two ratios were ~0.06 during the growing season (see Fig. 2).

	RMSE		Bias	
	10:00–12:00 hh	12:00–14:00 hh	10:00–12:00 hh	12:00–14:00 hh
US-Bo1	0.008	0.008	0.002	−0.003
DE-Geb	0.009	0.011	−0.006	−0.007
JP-Mas	0.009	0.007	0.007	0.000
KR-Hnm	0.010	0.008	0.006	0.002
US-Ne1	0.006	0.008	0.002	0.003
CA-Oas	0.008	0.009	0.001	−0.002
DE-Hai	0.012	0.013	−0.007	−0.009
US-MOz	0.010	0.009	−0.004	−0.002
US-Bar	0.027	0.030	−0.019	−0.022
IT-Ro1	0.008	0.006	−0.006	0.000
IT-Ro2	0.007	0.005	−0.006	−0.001
FR-Pue	0.011	0.007	−0.006	0.002
IT-Cpz	0.007	0.007	−0.003	0.001
AU-Tum	0.007	0.006	−0.002	0.002
ID-Pag	0.006	0.007	0.000	0.000
FI-Hyy	0.008	0.008	−0.005	−0.004
KR-Kw2	0.006	0.007	0.001	−0.002
NL-Loo	0.007	0.008	0.003	0.003
US-Blo	0.007	0.006	−0.002	−0.001
US-Me2	0.005	0.006	0.002	0.004
US-Me3	0.005	0.008	0.001	0.007
CH-Oe1	0.007	0.006	0.001	−0.001
NL-Ca1	0.006	0.007	0.001	−0.002
US-Var	0.008	0.008	0.000	−0.003
CA-Let	0.007	0.007	−0.003	−0.004
DE-Meh	0.008	0.011	−0.002	−0.009
US-Snd	0.003	0.004	0.002	−0.003
BE-Vie	0.015	0.013	−0.003	−0.006
CA-Gro	0.007	0.008	0.001	−0.001
CA-WP1	0.007	0.008	−0.002	−0.005
US-SRM	0.009	0.013	0.001	0.010
US-SO2	0.007	0.010	0.004	0.007
AU-How	0.011	0.008	0.008	0.005
US-Ton	0.008	0.010	0.003	0.002

The R_{gPOT} can be easily calculated with only a few basic pieces of information on the sun–Earth geometry (Liu and Jordan, 1960):

$$R_{gPOT} = S_{sc} \times \left[1 + 0.033 \cos\left(\frac{2\pi t_d}{365}\right)\right] \cos\beta \quad (1)$$

where S_{sc} is the solar constant (1360 W m^{-2}) (Kopp and Lean, 2011), t_d is the day of year, and β is solar zenith angle that is calculated following Michalsky (1988).

Our hypothesis allows us to develop the following relation:

$$SF_d(t) = \frac{1800\ \text{s} \times \lambda E(t)}{\int_d \lambda E(t)dt} \approx \frac{1800\ \text{s} \times R_{gPOT}(t)}{\int_d R_{gPOT}(t)dt} \quad (2)$$

where $SF_d(t)$ is the upscaling factor for a particular day ($_d$) of the year and function of the time t of the instantaneous λE. The 1800 s is the number of seconds in 30 min. Then the 8-day mean daily sum λE is:

$$\lambda E_{8day} = \frac{1}{8}\sum_{d=1}^{8} \frac{1800\ \text{s} \times \lambda E(t_d)}{SF_d(t_d)} \quad (3)$$

where the time of the snapshot, t_d, may change between one day and another according to the satellite passages.

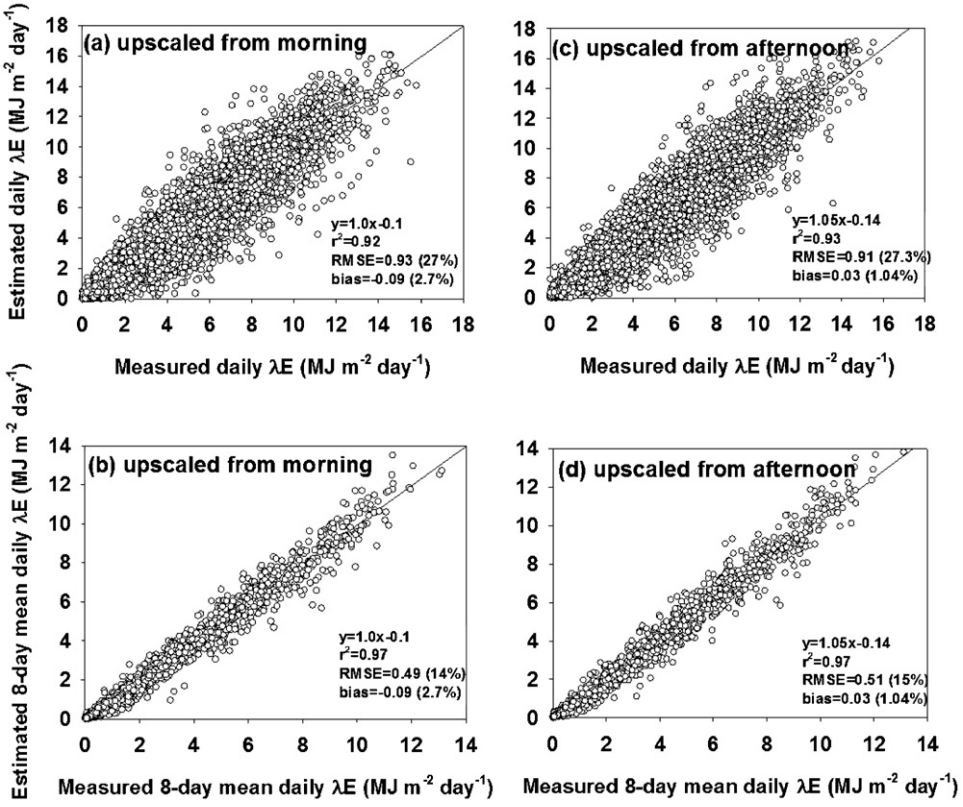

Fig. 3. Test of new scheme proposed in this study (Eqs. (2) and (3)) using 34 flux tower data. (a) Comparison between upscaled daily λE from a randomly selected half-hourly λE in the morning (10:00–12:00 hh) and measured daily λE. (b) Same with (a) except for 8-day mean daily scale. (c) Same with (a) except for selecting afternoon (12:00–14:00 hh). (d) Same with (c) except for using 8-day mean daily scale.

3. Results and discussions

3.1. Testing the constant evaporative fraction approach

We tested the constant *EF* approach using the flux tower data (Fig. 1). We randomly selected a half-hourly *E* data in the morning (10:00–12:00 hh) or in the afternoon (12:00–14:00 hh) to follow satellite overpass in the morning (Fig. 1a and c) or afternoon (Fig. 1b and d), upscaled to daily *E* using the constant *EF*, then averaged over 8-day intervals for all 34 sites. On daily *E*, we found that the constant *EF* approach caused −13% relative bias (the ratio of bias to the mean) with 49% relative root mean square error, RMSE (the ratio of RMSE to the mean) when upscaling from the morning data (Fig. 1a and c), and −7% relative bias and 103% relative RMSE when upscaling from the afternoon data (Fig. 1b and d). On 8-day mean daily *E*, relative RMSE from the morning data and from the afternoon data was reduced to 34% and 42%, respectively. Thus the constant *EF* approach will cause systematic underestimation of *E* by up to 13% with relative RMSE up to 42%.

The decrease of absolute relative bias in the afternoon indicates the *EF* tends to increase in the afternoon as observed in several studies (Brutsaert and Sugita, 1992; Sugita and Brutsaert, 1991). Some authors introduced a correction factor to account for non-constant *EF*. For example, a factor of 1.1 was multiplied with the *EF* to compensate for the 10% underestimation of daily *E* when using the morning satellite data (Anderson et al., 1997, 2007). Fig. 1a shows that such a correction could be made and 1.13 will be a better correction factor if using morning satellite data. However, the correction factor should be different in the morning and afternoon, which makes the constant *EF* approach more empirical and, therefore, much less useful.

3.2. Comparison between $R_{gPOT\_0.5\,h}/R_{gPOT\_day}$ and $\lambda E_{0.5\,h}/\lambda E_{day}$

We tested how the upscaling factor (Eq. (2)) varies across a range of PFT and climatic zones over the course of a year using the flux tower data (Fig. 2). The comparison between $R_{gPOT\_0.5\,h}/R_{gPOT\_day}$ and $\lambda E_{0.5\,h}/\lambda E_{day}$ over all sites between morning (10:00–12:00 hh) and afternoon (12:00–14:00 hh) during the growing season appears in Table 2. The mean RMSE and bias between $R_{gPOT\_0.5\,h}/R_{gPOT\_day}$ and $\lambda E_{0.5\,h}/\lambda E_{day}$ was 0.009 and −0.001 during the growing season. The RMSE and bias did not show pronounced asymmetry between in the morning and afternoon (Table 2). For simplicity and to capture the range in β, we randomly selected one site per each PFT, and reported for 10:00–10:30 hh and 11:30–12:00 hh in Fig. 2. Overall, the scaling factor *SF* computed from the R_{gPOT} and measured *E* showed similar seasonal patterns and magnitude among sites. Some sites showed discrepancy between $R_{gPOT\_0.5\,h}/R_{gPOT\_day}$ and $\lambda E_{0.5\,h}/\lambda E_{day}$ in winter when *E* is very small, which caused numerical instability in the $\lambda E_{0.5\,h}/\lambda E_{day}$ (see FI-Hyy site in Fig. 2). The seasonal variations of $R_{gPOT\_0.5\,h}/R_{gPOT\_day}$ and $\lambda E_{0.5\,h}/\lambda E_{day}$ should be noted. The constant scaling factor approach like Sims et al. (2005) is likely error prone as the $\lambda E_{0.5\,h}/\lambda E_{day}$ shows seasonal pattern. The *SF* varied with day length and it was lower at times and places with longer days and higher in times and places with shorter days. In fact, the tropical site (ID-Pag) showed less seasonality because the length of day does not change much over the year. On the other hand, northern sites showed distinct seasonality with the lowest ratios during summer when day length is the longest (e.g. FI-Hyy and CA-Wp1).

3.3. Evaluation of upscaling scheme using flux tower data

We tested the efficacy of the upscaling scheme that converts half-hourly *E* to daily *E* or 8-day mean daily *E* using the

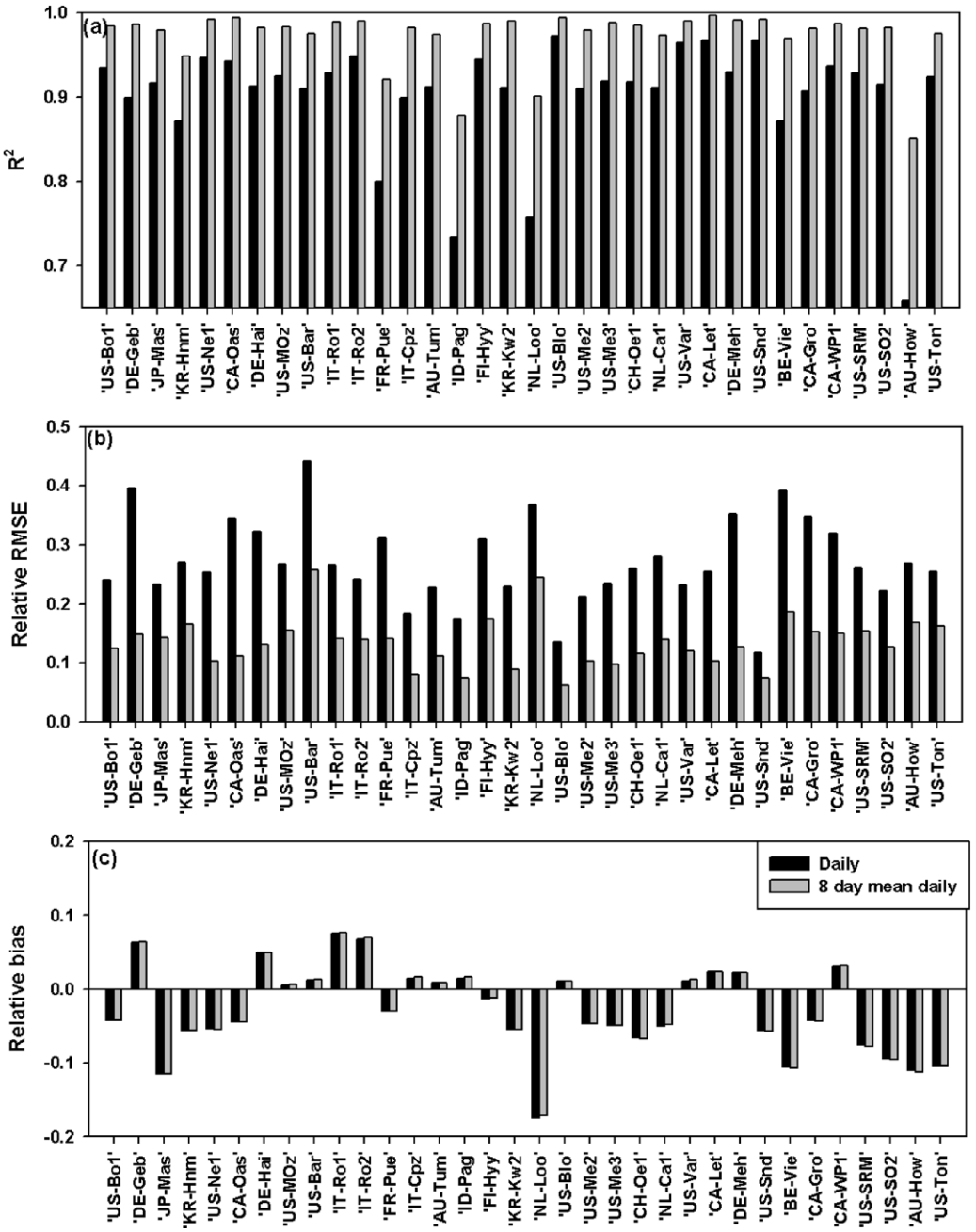

Fig. 4. Statistics for comparison between upscaled daily (or 8-day mean daily) λE from a randomly selected half-hourly λE in the morning (10:00–12:00 hh) and measured daily (or 8-day mean daily) λE for 34 flux tower sites. The 34 flux tower data were used, and the upscaling equations appear in Eqs. (2) and (3). (a) Determinant coefficient (r^2). (b) Relative root mean square error (RMSE). (c) Relative bias.

flux tower data of all 34 sites. First, we compared the upscaled daily E from a randomly selected half-hourly E in the morning (10:00–12:00 hh) and a randomly selected half-hourly E in the afternoon (12:00–14:00 hh) against the measured daily E (Fig. 3a and c). Both cases showed highly linear relations among half-hourly E and measured daily E (r^2 = 0.92 and 0.93 for upscaled from morning and afternoon, respectively). Next, we compared the 8-day mean daily E upscaled from morning or afternoon against measured 8-day mean daily E (Fig. 3b and d). Averaging daily E over an 8-day period greatly reduced the RMSE by about 50%. The upscaled E from morning and upscaled E from afternoon showed relative RMSE < 15% with absolute relative bias < 2.7% compared to the measured 8-day mean daily E. This opens the possibility to only use either morning satellite (i.e., Terra) or afternoon satellite (i.e., Aqua) to upscale instantaneous E to an 8-day mean daily E. Hereinafter, we restrict our analysis to the morning data. It is notable that the constant EF approach required using different correction factors for morning and afternoon.

We evaluated the performance of the upscaling scheme at the site level (Fig. 4). We randomly sampled a half-hourly flux tower E between 10:00 hh and 12:00 hh per day, and upscaled to daily E. We compared the measured and upscaled E for the daily and 8-day mean daily cases. At daily scale, the tropical sites showed relatively low r^2 (0.75 and 0.66 for ID-Pag and AU-How, respectively), presumably due to irregular cloudiness. However, averaging daily E over 8-day periods improved the r^2 to 0.82 and

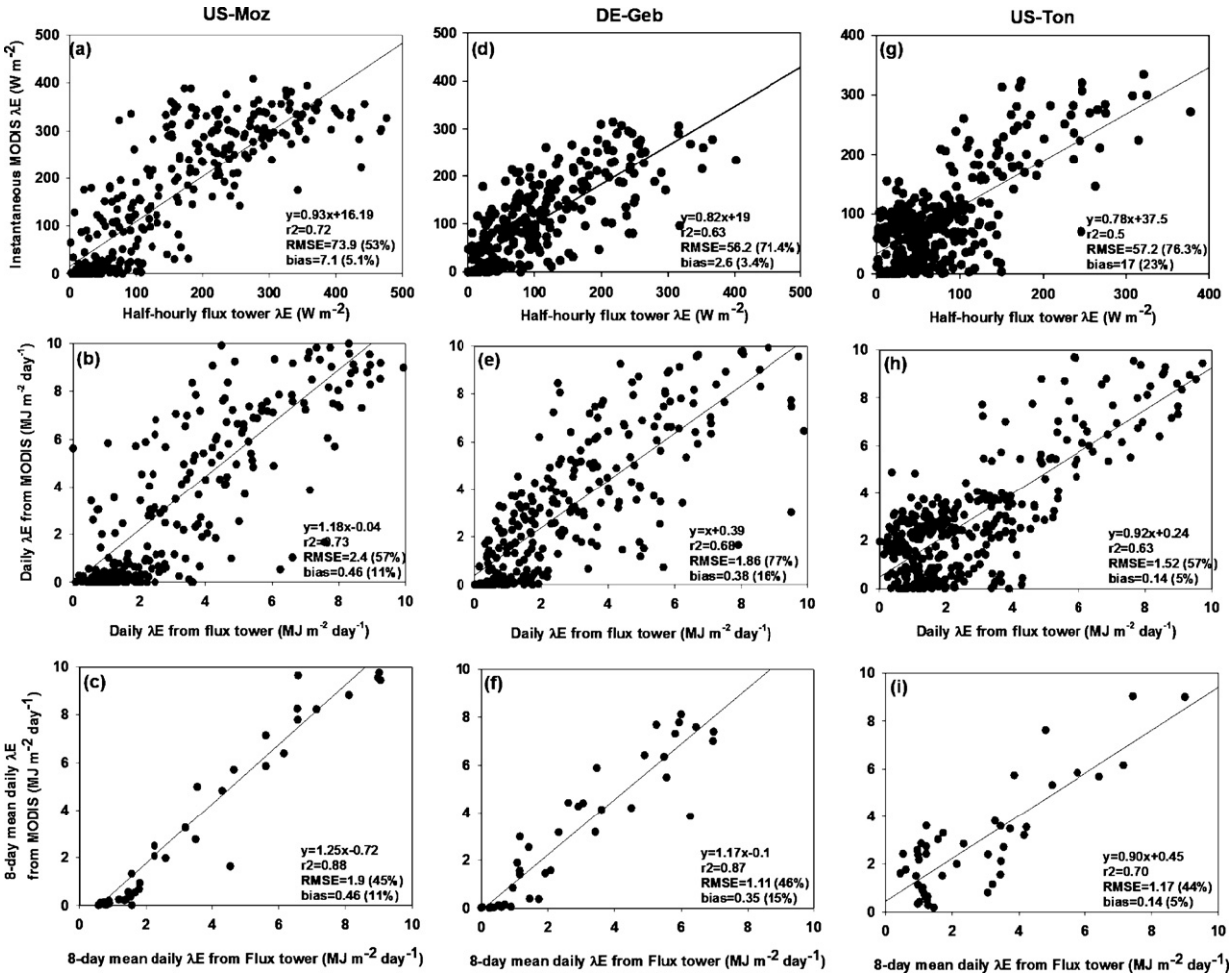

Fig. 5. Comparison between MODIS derived instantaneous λE (Ryu et al., 2011) and half-hourly flux tower λE (a, d, and g), comparison between upscaled daily E from MODIS using Eq. (2) and daily E from flux tower (b, e, and h), and comparison between 8-day mean daily E from MODIS using Eq. (3) and 8-day mean daily E from flux tower (c, f, and i). Three sites were selected. (a–c) US-Moz. (d–f) DE-Geb. (g–i) US-Ton.

0.89 for ID-Pag and AU-How, respectively. Overall, the testing of upscaled 8-day mean daily E against the measurement showed $r^2 > 0.88$, relative RMSE < 30%, absolute relative bias < 17% for the all sites.

3.4. Applying the upscaling scheme to a MODIS-derived E model

We employed the upscaling scheme to scale-up MODIS Terra derived snap-shot E (10:00–12:00 hh) over 8-day to an 8-day mean daily E. We assumed that the instantaneous E represents the half-hourly mean E, and applied the upscaling scheme (Eq. (3)). We tested three sites in Fig. 4c that showed little bias (US-MOz, 0.3%), positive bias (DE-Geb, 6.7%), and negative bias (US-Ton, −10%). We compared three steps: (1) instantaneous E from MODIS and half-hourly E from flux tower (Fig. 5a, d, and g), (2) upscaled daily E from MODIS using Eq. (2) and daily E from flux tower (Fig. 5b, e, and h), and (3) 8-day mean daily E from MODIS using Eq. (3) and 8-day mean daily E from flux tower (Fig. 5c, f, and i). When comparing the 1st and 2nd steps, we found that the changes of relative biases are notable, which is related with the inherent biases in the upscaling factor for each site (Fig. 4c). Overall, the r^2 and relative RMSE did not change much between the 1st and 2nd steps but they were improved in the 3rd step. This indicates that the random errors were not removed much in the daily upscaling scheme (Eq. (2)), but they were largely removed in averaging the upscaled daily E over an 8-day interval (Eq. (3)).

As the characteristics of the upscaling scheme appeared in Fig. 4c (increase of r^2, reduction of RMSE between daily and 8-day mean daily scale, and inherent bias) was reflected in Fig. 5, we conclude that the upscaling scheme is applicable to upscale the instantaneous MODIS-E within an 8-day interval to an 8-day mean daily E.

3.5. Sources of uncertainty in the upscaling scheme

We restricted the uncertainty sources for the upscaling scheme when using flux tower data only. The MODIS derived E includes many other uncertainties such as the uncertainty in the E model, MODIS data, and footprint mismatch, which are all not directly related with the upscaling scheme. The proposed upscaling scheme assumed that mean diurnal variation of R_{gPOT} over an 8-day scales with the mean diurnal variation of E over an 8-day period. This assumption will be violated if (1) there is considerable nighttime E (Dawson et al., 2007; Novick et al., 2009; Tolk et al., 2006) and (2) there is asymmetry of E between morning and afternoon (Wilson et al., 2002). In fact, several sites showed substantial nighttime E. For example, the annual sum of nighttime E constituted 10% of the annual sum of E in the JP-Mas site. On the other hand, annual sum of nighttime E at the DE-Hai site was −9% (e.g. dew formation) of the annual sum E. The presence of positive (negative) nighttime E caused negative (positive) biases in the upscaling scheme (see Fig. 4c). However, we note that the nighttime E measured from

eddy covariance system might be error-prone due to low turbulence (Fisher et al., 2007).

The asymmetry of diurnal variation of *E* was observed at several sites. For example, IT-RO1 and FR-Pue sites experienced drought stress during the growing season, thus *E* was higher in the morning than in the afternoon, which is common for summer drought affected forests (e.g. semi-arid forests and woodlands) (Tognetti et al., 1999; White et al., 2000). In contrast, two rice paddy sites (JP-Mas and KR-Hnm) showed higher *E* in the afternoon than in the morning during the growing season because of no water limitation due to irrigation and higher vapor pressure deficit in the afternoon. Other causes of asymmetry may be originated by the discontinuous presence of clouds during the day. As we upscaled *E* from morning data, higher (lower) *E* in the morning than in the afternoon caused overestimation (underestimation) of upscaled *E*. Overall, however, the biases influenced by the asymmetry in these sites were less than 10% on an annual scale (Fig. 4c). As we found in Section 3.2, the upscaling scheme is error-prone when *E* is very small (e.g. winter in high latitudes, see CA-WP1 and FI-Hyy in Fig. 2). However, the impact of this uncertainty to a daily or 8-daily mean daily sum *E* is likely marginal as the winter *E* is very small.

We checked the impact of energy imbalance on the performance of our approach (Eqs. (2) and (3)) and constant *EF* approach, and found that the impact was not substantial. For daily *E* calculated from morning data where energy balance closure had been applied, relative RMSE and bias error in our approach were 27.3% (27%) and 1% (2.7%), respectively where the values in brackets were derived using original flux data appeared in Fig. 3a. The relative RMSE and bias errors in the constant *EF* approach were 54.7% (49%) and −14% (−13%), respectively where the values in brackets were derived using original flux data appeared in Fig. 1a.

3.6. Application of the upscaling scheme to other variables

We tested the efficacy of the proposed upscaling scheme to the other variables such as GPP and solar irradiance. We randomly selected one half-hour flux tower data (GPP or solar irradiance) between 10:00 hh and 12:00 hh, upscaled to a daily sum by dividing by *SF* (Eq. (2)), then averaged the daily sum over an 8-day interval (Eq. (3)) for all 34 flux tower data. The upscaled 8-day mean daily GPP and solar irradiance showed excellent agreement with flux tower 8-day mean daily GPP (0.98 r^2, 0.44% RMSE, −0.09% bias, Fig. 6a) and solar irradiance (0.97 r^2, 11.89% RMSE, 6.89% bias, Fig. 6b), respectively.

We compared our approach with the one of Sims et al. (2005) for GPP (Fig. 7). Sims et al. (2005) proposed a consistent linear regression equation: $y = 9.14x - 12.2$ where y is 8-daily mean daily GPP (mmol m^{-2} day^{-1}), and x is mid-day hourly GPP. The authors tested 8 flux tower sites that located in a relatively narrow latitude range between 38.4°N and 49.7°N. Here we applied both approaches to a further north located flux site, FI-Hyy (61.8°N). In this case, the Sims et al. (2005) approach showed a curvilinear relation with negative bias (−15%) whereas our approach showed a linear relation with little bias (−3%) (Fig. 7). The curvilinear relation in the Sims et al. (2005) was expected as the upscaling factor varied over the season (See FI-Hyy in Fig. 2). As our approach considers the seasonality of the scaling factor including the effect of latitude, it offers a more general upscaling scheme than the consistent linear regression approach (Sims et al., 2005).

3.7. Advantages of the proposed upscaling scheme

The proposed upscaling scheme has several important advantages over the constant *EF* ratio approach and the consistent linear relation approach (Sims et al., 2005). While our approach requires only a few basic inputs (latitude, longitude and time (see Eq. (1))),

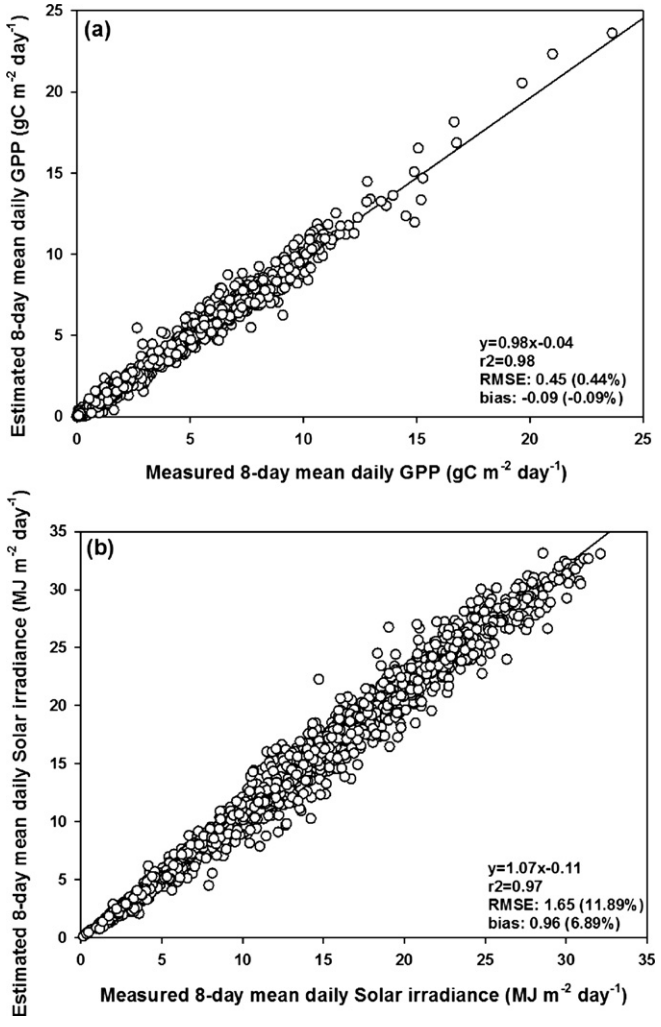

Fig. 6. Test of the proposed upscaling scheme to (a) GPP and (b) solar irradiance using the 34 flux tower data. Comparison between upscaled 8-day mean daily sum GPP (or solar irradiance) from a randomly selected half-hourly λE in the morning (10:00–12:00 hh) and measured 8-day mean daily sum GPP (or solar irradiance).

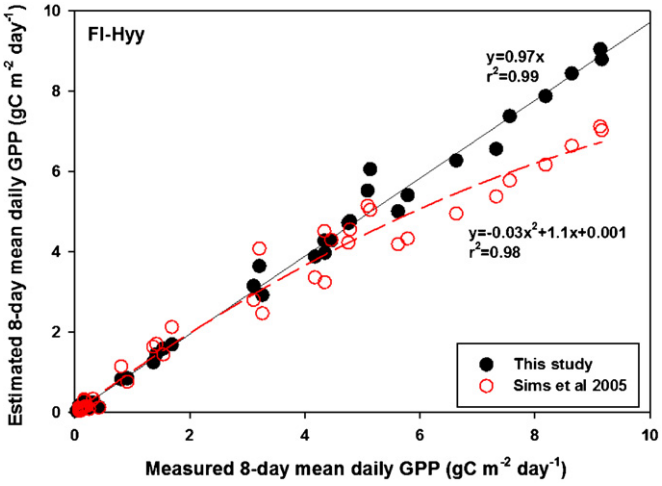

Fig. 7. Comparison of 8-day mean daily GPP between flux tower data and two upscaling schemes that include Sims et al. (2005) and our upscaling approach (Eqs. (2) and (3)) for FI-Hyy site.

the constant *EF* approach requires calculating instantaneous and daytime integrated R_n and G. Furthermore, the daytime integrated R_n is only available at coarse resolution such as GOES (20 km). The constant *EF* approach required using different correction factors for morning and afternoon (Fig. 1), whereas it was not necessary to use the correction factors in our approach. All statistical evaluations (r^2, RMSE and bias) were superior for our approach than the constant *EF* approach (Figs. 1 and 3). Our simple approach explicitly considered the sun–Earth geometry, which enabled us to capture the seasonality of the scaling factor. This outperformed the consistent linear regression approach (see Fig. 7). Thus our simple approach offers a very simple, general way to upscale instantaneous estimates to the 8-daily mean daily estimates although the proposed approach is likely error prone in biomes that showed substantial nighttime E (e.g. JP-Mas site) or water extremes (e.g. woodlands and forests experiencing seasonal drought, or rice paddy, See 3.5) due to asymmetry of diurnal variation in E.

4. Summary and conclusions

We presented a temporal upscaling scheme for E from instantaneous measurements near mid-day to 8-day mean values by using the ratio of half-hourly R_{gPOT} to the daily sum R_{gPOT} (Eq. (3)). Based on the data from 34 flux tower sites, we found that the upscaled 8-day mean daily E showed a clear linear relation ($r^2 = 0.97$), good agreement (relative RMSE = 14%) and little bias (−2.7%) with the observed 8-day daily E using flux tower data only. At the individual site level, the upscaling-scheme derived E showed $r^2 > 0.88$, relative RMSE < 30%, absolute relative bias < 17% against flux tower data. The upscaling factor showed pronounced seasonal patterns in the sites located in high latitudes whereas it showed less seasonal pattern in the tropical sites, which were caused by the sun–Earth geometry (see Fig. 2). We coupled the upscaling scheme with the MODIS-derived E model (Ryu et al., 2011), and found that the upscaling scheme allowed us to reliably upscale instantaneous E to an 8-day mean daily E. Also, our scheme could be used to upscale GPP and solar irradiance as well (see Fig. 6). The constant *EF* approach which has been commonly used to extrapolate instantaneous E to daily sum E systematically underestimate daily E (−8 to −13%) based on the 34 flux tower data. The proposed scheme was less successful in regions that experienced substantial nighttime E or asymmetry of diurnal variation in E due to water stress (see Section 3.5), and this needs to be taken into consideration in regional and global applications of the method. Our scheme will contribute to reducing uncertainty in continuous monitoring of hydrological cycle with remote sensing.

Acknowledgements

This work used eddy covariance data acquired by the FLUXNET community and in particular by the following networks: AmeriFlux (U.S. Department of Energy, Biological and Environmental Research, Terrestrial Carbon Program (DE-FG02-04ER63917 and DE-FG02-04ER63911)), AfriFlux, AsiaFlux, CarboAfrica, CarboEuropeIP, CarboItaly, CarboMont, ChinaFlux, Fluxnet-Canada (supported by CFCAS, NSERC, BIOCAP, Environment Canada, and NRCan), GreenGrass, KoFlux (supported by Sustainable Water Resources Center of 21C Frontier Research Program Code: 1-8-3 Korea), LBA, NECC, OzFlux, TCOS-Siberia, USCCC. We acknowledge the financial support to the eddy covariance data harmonization provided by CarboEuropeIP, FAO-GTOS-TCO, iLEAPS, Max Planck Institute for Biogeochemistry, National Science Foundation, University of Tuscia, Universite Laval and Environment Canada and US Department of Energy and the database development and technical support from Berkeley Water Center, Lawrence Berkeley National Laboratory, Microsoft Research eScience, Oak Ridge National Laboratory, University of California – Berkeley, University of Virginia. YR was supported by NASA Headquarters under the NASA Earth and Space Science Fellowship Program (NNX08AU25H) and the Berkeley Water Center/Microsoft eScience project. MODIS data processing was supported by Microsoft Azure cloud computing service. Drs. Andrew Richardson, John Norman, Oliver Sonnentag and Paul Stoy gave insightful comments. Data from the Tonzi and Vaira Ranches are supported by the Office of Science (BER), US Department of Energy, Grant DE-FG02-06ER64308. Data from Metolius sites are supported by the Office of Science (BER), US Department of Energy, Grant DE-FG02-06ER64318. Data collection at the Lethbridge grassland and western peatland sites in Canada were supported by the Natural Sciences and Engineering Research Council of Canada, the Canadian Foundation for Climate and Atmospheric Sciences, and BIOCAP Canada.

References

Allard, V., Ourcival, J.M., Rambal, S., Joffre, R., Rocheteau, A., 2008. Seasonal and annual variation of carbon exchange in an evergreen Mediterranean forest in southern France. Global Change Biol. 14 (4), 714–725.

Ammann, C., Flechard, C.R., Leifeld, J., Neftel, A., Fuhrer, J., 2007. The carbon budget of newly established temperate grassland depends on management intensity. Agric. Ecosyst. Environ. 121 (1-2), 5–20.

Anderson, M.C., Norman, J.M., Diak, G.R., Kustas, W.P., Mecikalski, J.R., 1997. A two-source time-integrated model for estimating surface fluxes using thermal infrared remote sensing. Remote Sens. Environ. 60 (2), 195–216.

Anderson, M.C., Norman, J.M., Kustas, W.P., Houborg, R., Starks, P.J., Agam, N., 2008. A thermal-based remote sensing technique for routine mapping of land-surface carbon, water and energy fluxes from field to regional scales. Remote Sens. Environ. 112 (12), 4227–4241.

Anderson, M.C., Norman, J.M., Mecikalski, J.R., Otkin, J.A., Kustas, W.P., 2007. A climatological study of evapotranspiration and moisture stress across the continental United States based on thermal remote sensing. 1. Model formulation. J. Geophys. Res. 112 (D10117), doi:10.1029/2006JD007506.

Anthoni, P.M., Knohl, A., Rebmann, C., Freibauer, A., Mund, M., Ziegler, W., Kolle, O., Schulze, E.D., 2004. Forest and agricultural land-use-dependent CO_2 exchange in Thuringia, Germany. Global Change Biol. 10 (12), 2005–2019.

Aubinet, M., Chermanne, B., Vandenhaute, M., Longdoz, B., Yernaux, M., Laitat, E., 2001. Long term carbon dioxide exchange above a mixed forest in the Belgian Ardennes. Agric. For. Meteorol. 108 (4), 293–315.

Baldocchi, D.D., Ryu, Y., 2011. A synthesis of forest evaporation fluxes from days to years as measured with eddy covariance. In: Levia, D.F., Carlyle-Moses, D.E., Tanaka, T. (Eds.), Forest Hydrology and Biogeochemistry: Synthesis of Past Research and Future Directions. Springer-Verlag, Heidelberg, Germany.

Baldocchi, D.D., Xu, L.K., Kiang, N., 2004. How plant functional-type, weather, seasonal drought, and soil physical properties alter water and energy fluxes of an oak-grass savanna and an annual grassland. Agric. For. Meteorol. 123 (1-2), 13–39.

Beringer, J., Hutley, L.B., Tapper, N.J., Cernusak, L.A., 2007. Savanna fires and their impact on net ecosystem productivity in North Australia. Global Change Biol. 13 (5), 990–1004.

Brauman, K.A., Daily, G.C., Duarte, T.K., Mooney, H.A., 2007. The nature and value of ecosystem services: an overview highlighting hydrologic services. Annu. Rev. Environ. Resour. 32, 67–98.

Brutsaert, W., Sugita, M., 1992. Application of self-preservation in the diurnal evolution of the surface-energy budget to determine daily evaporation. J. Geophys. Res. 97 (D17), 18377–18382.

Collatz, G.J., Ball, J.T., Grivet, C., Berry, J.A., 1991. Physiological and environmental regulation of stomatal conductance, photosynthesis and transpiration: a model that includes a laminar boundary layer. Agric. For. Meteorol. 54, 107–136.

Crago, R.D., 1996. Conservation and variability of the evaporative fraction during the daytime. J. Hydrol. 180 (1–4), 173–194.

Dawson, T.E., Burgess, S.S.O., Tu, K.P., Oliveira, R.S., Santiago, L.S., Fisher, J.B., Simonin, K.A., Ambrose, A.R., 2007. Nighttime transpiration in woody plants from contrasting ecosystems. Tree Physiol. 27 (4), 561–575.

dePury, D.G.G., Farquhar, G.D., 1997. Simple scaling of photosynthesis from leaves to canopies without the errors of big-leaf models. Plant Cell Environ. 20 (5), 537–557.

Detto, M., Baldocchi, D.D., Katul, G., 2010. Scaling properties of biologically active scalar concentration fluctuations in the surface boundary layer over a managed peatland. Boundary Layer Meteorol., doi:10.1007/s10546-010-9514-z.

Diak, G.R., Mecikalski, J.R., Anderson, M.C., Norman, J.M., Kustas, W.P., Torn, R.D., DeWolf, R.L., 2004. Estimating land surface energy budgets from space: review and current efforts at the University of Wisconsin—Madison and USDA–ARS. Bull. Am. Meteorol. Soc. 85 (1), 65–78.

Dolman, A.J., Moors, E.J., Elbers, J.A., 2002. The carbon uptake of a mid latitude pine forest growing on sandy soil. Agric. For. Meteorol. 111 (3), 157–170.

Ferguson, C.R., Sheffield, J., Wood, E.F., Gao, H.L., 2010. Quantifying uncertainty in a remote sensing-based estimate of evapotranspiration over continental USA. Int. J. Remote Sens. 31 (14), 3821–3865.
Fisher, J.B., Baldocchi, D.D., Misson, L., Dawson, T.E., Goldstein, A.H., 2007. What the towers don't see at night: nocturnal sap flow in trees and shrubs at two AmeriFlux sites in California. Tree Physiol. 27 (4), 597–610.
Fisher, J.B., Tu, K.P., Baldocchi, D.D., 2008. Global estimates of the land-atmosphere water flux based on monthly AVHRR and ISLSCP-II data, validated at 16 FLUXNET sites. Remote Sens. Environ. 112 (3), 901–919.
Flanagan, L.B., Wever, L.A., Carlson, P.J., 2002. Seasonal and interannual variation in carbon dioxide exchange and carbon balance in a northern temperate grassland. Global Change Biol. 8 (7), 599–615.
Goldstein, A.H., Hultman, N.E., Fracheboud, J.M., Bauer, M.R., Panek, J.A., Xu, M., Qi, Y., Guenther, A.B., Baugh, W., 2000. Effects of climate variability on the carbon dioxide, water, and sensible heat fluxes above a ponderosa pine plantation in the Sierra Nevada (CA). Agric. For. Meteorol. 101 (2-3), 113–129.
Gu, L.H., Meyers, T., Pallardy, S.G., Hanson, P.J., Yang, B., Heuer, M., Hosman, K.P., Liu, Q., Riggs, J.S., Sluss, D., Wullschleger, S.D., 2007. Influences of biomass heat and biochemical energy storages on the land surface fluxes and radiative temperature. J. Geophys. Res. 112 (D02107), doi:10.1029/2006JD007425.
Held, I.M., Soden, B.J., 2000. Water vapor feedback and global warming. Annu. Rev. Energy Environ. 25, 441–475.
Hirano, T., Segah, H., Harada, T., Limin, S., June, T., Hirata, R., Osaki, M., 2007. Carbon dioxide balance of a tropical peat swamp forest in Kalimantan, Indonesia. Global Change Biol. 13 (2), 412–425.
Hong, J., Kim, J., Lee, D., Lim, J.H., 2008. Estimation of the storage and advection effects on H_2O and CO_2 exchanges in a hilly KoFlux forest catchment. Water Resour. Res. 44 (W01426), doi:10.1029/2007WR006408.
IPCC, 2007. Climate Change 2007: The physical science basis. In: Solomon, S., et al. (Eds.), Contribution of Working Group I to the Fourth Assessment Report of the Intergovernmental Panel on Climate Change. Cambridge University Press, Cambridge, United Kingdom and New York, NY, USA.
Iwabuchi, H., 2006. Efficient Monte Carlo methods for radiative transfer modeling. J. Atmos. Sci. 63 (9), 2324–2339.
Jackson, R.D., Hatfield, J.L., Reginato, R.J., Idso, S.B., Pinter Jr., P.J., 1983. Estimation of daily evapotranspiration from one time-of-day measurements. Agric. Water Manage. 7 (1–3), 351–362.
Jacobs, C.M.J., Jacobs, A.F.G., Bosveld, F.C., Hendriks, D.M.D., Hensen, A., Kroon, P.S., Moors, E.J., Nol, L., Schrier-Uijl, A., Veenendaal, E.M., 2007. Variability of annual CO_2 exchange from Dutch grasslands. Biogeosciences 4 (5), 803–816.
Kattge, J., Knorr, W., Raddatz, T., Wirth, C., 2009. Quantifying photosynthetic capacity and its relationship to leaf nitrogen content for global-scale terrestrial biosphere models. Global Change Biol. 15, 976–991.
Kobayashi, H., Iwabuchi, H., 2008. A coupled 1-D atmosphere and 3-D canopy radiative transfer model for canopy reflectance, light environment, and photosynthesis simulation in a heterogeneous landscape. Remote Sens. Environ. 112 (1), 173–185.
Kopp, G., Lean, J.L., 2011. A new, lower value of total solar irradiance: evidence and climate significance. Geophys. Res. Lett. 38 (L01706), doi:10.1029/2010gl045777.
Krishnan, P., Black, T.A., Grant, N.J., Barr, A.G., Hogg, E.T.H., Jassal, R.S., Morgenstern, K., 2006. Impact of changing soil moisture distribution on net ecosystem productivity of a boreal aspen forest during and following drought. Agric. For. Meteorol. 139 (3-4), 208–223.
Kutsch, W.L., Kolle, O., Rebmann, C., Knohl, A., Ziegler, W., Schulze, E.D., 2008. Advection and resulting CO_2 exchange uncertainty in a tall forest in central Germany. Ecol. Appl. 18 (6), 1391–1405.
Leuning, R., Cleugh, H.A., Zegelin, S.J., Hughes, D., 2005. Carbon and water fluxes over a temperate Eucalyptus forest and a tropical wet/dry savanna in Australia: measurements and comparison with MODIS remote sensing estimates. Agric. For. Meteorol. 129, 151–173.
Leuning, R., Raupach, M.R., Coppin, P.A., Cleugh, H.A., Isaac, P., Denmead, O.T., Dunin, F.X., Zegelin, S., Hacker, J., 2004. Spatial and temporal variations in fluxes of energy, water vapour and carbon dioxide during OASIS 1994 and 1995. Boundary Layer Meteorol. 110 (1), 3–38.
Liu, B.Y.H., Jordan, R.C., 1960. The interrelationship and characteristic distribution of direct, diffuse and total solar radiation. Solar Energy 4 (3), 1–19.
Loveland, T.R., Reed, B.C., Brown, J.F., Ohlen, D.O., Zhu, Z., Yang, L., Merchant, J.W., 2000. Development of a global land cover characteristics database and IGBP DISCover from 1 km AVHRR data. Int. J. Remote Sens. 21 (6-7), 1303–1330.
Luo, H.Y., Oechel, W.C., Hastings, S.J., Zulueta, R., Qian, Y.H., Kwon, H., 2007. Mature semiarid chaparral ecosystems can be a significant sink for atmospheric carbon dioxide. Global Change Biol. 13 (2), 386–396.
Masuoka, E., Fleig, A., Wolfe, R.E., Patt, F., 1998. Key characteristics of MODIS data products. IEEE Trans. Geosci. Remote Sens. 36 (4), 1313–1323.
McCaughey, J.H., Pejam, M.R., Arain, M.A., Cameron, D.A., 2006. Carbon dioxide and energy fluxes from a boreal mixedwood forest ecosystem in Ontario, Canada. Agric. For. Meteorol. 140 (1–4), 79–96.
Meyers, T.P., Hollinger, S.E., 2004. An assessment of storage terms in the surface energy balance of maize and soybean. Agric. For. Meteorol. 125 (1–2), 105–115.
Michalsky, J.J., 1988. The astronomical-almanacs algorithm for approximate solar position (1950–2050). Solar Energy 40 (3), 227–235.
Nishida, K., Nemani, R.R., Running, S.W., Glassy, J.M., 2003. An operational remote sensing algorithm of land surface evaporation. J. Geophys. Res. 108 (D9), 4270, doi:10.1029/2002JD002062.
Novick, K.A., Oren, R., Stoy, P.C., Siqueira, M.B.S., Katul, G.G., 2009. Nocturnal evapotranspiration in eddy-covariance records from three co-located ecosystems in the Southeastern US: implications for annual fluxes. Agric. For. Meteorol. 149 (9), 1491–1504.
Ollinger, S.V., Richardson, A.D., Martin, M.E., Hollinger, D.Y., Frolking, S.E., Reich, P.B., Plourde, L.C., Katul, G.G., Munger, J.W., Oren, R., Smith, M.L., Paw U, K.T., Bolstad, P.V., Cook, B.D., Day, M.C., Martin, T.A., Monson, R.K., Schmid, H.P., 2008. Canopy nitrogen, carbon assimilation, and albedo in temperate and boreal forests: functional relations and potential climate feedbacks. Proc. Natl. Acad. Sci. U.S.A. 105 (49), 19336–19341.
Paw U, K.T., Gao, W.G., 1988. Applications of solutions to non-linear energy budget equations. Agric. For. Meteorol. 43 (2), 121–145.
Pisek, J., Chen, J.M., Lacaze, R., Sonnentag, O., Alikas, K., 2010. Expanding global mapping of the foliage clumping index with multi-angular POLDER three measurements: evaluation and topographic compensation. ISPRS-J. Photogramm. Remote Sens. 65 (4), 341–346.
Prata, A.J., 1996. A new long-wave formula for estimating downward clear-sky radiation at the surface. Q. J. R. Meteorol. Soc. 122 (533), 1127–1151.
Raupach, M.R., 1998. Influences of local feedbacks on land-air exchanges of energy and carbon. Global Change Biol. 4 (5), 477–494.
Reichstein, M., Ciais, P., Papale, D., Valentini, R., Running, S., Viovy, N., Cramer, W., Granier, A., Ogee, J., Allard, V., Aubinet, M., Bernhofer, C., Buchmann, N., Carrara, A., Grunwald, T., Heimann, M., Heinesch, B., Knohl, A., Kutsch, W., Loustau, D., Manca, G., Matteucci, G., Miglietta, F., Ourcival, J.M., Pilegaard, K., Pumpanen, J., Rambal, S., Schaphoff, S., Seufert, G., Soussana, J.F., Sanz, M.J., Vesala, T., Zhao, M., 2007. Reduction of ecosystem productivity and respiration during the European summer 2003 climate anomaly: a joint flux tower, remote sensing and modelling analysis. Global Change Biol. 13 (3), 634–651.
Reichstein, M., Falge, E., Baldocchi, D., Papale, D., Aubinet, M., Berbigier, P., Bernhofer, C., Buchmann, N., Gilmanov, T., Granier, A., Grunwald, T., Havrankova, K., Ilvesniemi, H., Janous, D., Knohl, A., Laurila, T., Lohila, A., Loustau, D., Matteucci, G., Meyers, T., Miglietta, F., Ourcival, J.M., Pumpanen, J., Rambal, S., Rotenberg, E., Sanz, M., Tenhunen, J., Seufert, G., Vaccari, F., Vesala, T., Yakir, D., Valentini, R., 2005. On the separation of net ecosystem exchange into assimilation and ecosystem respiration: review and improved algorithm. Global Change Biol. 11 (9), 1424–1439.
Richardson, A.D., Jenkins, J.P., Braswell, B.H., Hollinger, D.Y., Ollinger, S.V., Smith, M.L., 2007. Use of digital webcam images to track spring green-up in a deciduous broadleaf forest. Oecologia 152 (2), 323–334.
Ryu, Y., Baldocchi, D.D., Kobayashi, H., van Ingen, C., Li, J., Black, T.A., Beringer, J., van Gorsel, E., Knohl, A., Law, B.E., Roupsard, O., 2011. Integration of MODIS land and atmosphere products with a coupled-process model to estimate gross primary productivity and evapotranspiration from 1 km to global scales. Global Biogeochem. Cycles, in press.
Ryu, Y., Baldocchi, D.D., Ma, S., Hehn, T., 2008a. Interannual variability of evapotranspiration and energy exchanges over an annual grassland in California. J. Geophys. Res. 113 (D09104), doi:10.1029/2007JD009263.
Ryu, Y., Kang, S., Moon, S.K., Kim, J., 2008b. Evaluation of land surface radiation balance derived from Moderate Resolution Imaging Spectrometer (MODIS) over complex terrain and heterogeneous landscape on clear sky days. Agric. For. Meteorol. 148 (10), 1538–1552.
Ryu, Y., Nilson, T., Kobayashi, H., Sonnentag, O., Law, B.E., Baldocchi, D.D., 2010a. On the correct estimation of effective leaf area index: does it reveal information on clumping effects? Agric. For. Meteorol. 150 (3), 463–472.
Ryu, Y., Sonnentag, O., Nilson, T., Vargas, R., Kobayashi, H., Wenk, R., Baldocchi, D.D., 2010b. How to quantify tree leaf area index in a heterogeneous savanna ecosystem: a multi-instrument and multi-model approach. Agric. For. Meteorol. 150 (1), 63–76.
Saito, M., Miyata, A., Nagai, H., Yamada, T., 2005. Seasonal variation of carbon dioxide exchange in rice paddy field in Japan. Agric. For. Meteorol. 135 (1–4), 93–109.
Schaaf, C.B., Gao, F., Strahler, A.H., Lucht, W., Li, X., Tsang, T., Strugnell, N.C., Zhang, X., Jin, Y., Muller, J.-P., 2002. First operational BRDF, albedo nadir reflectance products from MODIS. Remote Sens. Environ. 83 (1–2), 135–148.
Scherer-Lorenzen, M., Schulze, E.D., Don, A., Schumacher, J., Weller, E., 2007. Exploring the functional significance of forest diversity: a new long-term experiment with temperate tree species (BIOTREE). Perspect. Plant Ecol. Evolut. Syst. 9 (2), 53–70.
Scott, R.L., Jenerette, G.D., Potts, D.L., Huxman, T.E., 2009. Effects of seasonal drought on net carbon dioxide exchange from a woody-plant-encroached semiarid grassland. J. Geophys. Res.-Biogeosci. 114 (G04004), doi:10.1029/2008JG000900.
Sims, D.A., Rahman, A.F., Cordova, V.D., Baldocchi, D.D., Flanagan, L.B., Goldstein, A.H., Hollinger, D.Y., Misson, L., Monson, R.K., Schmid, H.P., Wofsy, S.C., Xu, L.K., 2005. Midday values of gross CO_2 flux and light use efficiency during satellite overpasses can be used to directly estimate eight-day mean flux. Agric. For. Meteorol. 131 (1-2), 1–12.
Sugita, M., Brutsaert, W., 1991. Daily evaporation over a region from lower boundary-layer profiles measured with radiosondes. Water Resour. Res. 27 (5), 747–752.
Suni, T., Rinne, J., Reissell, A., Altimir, N., Keronen, P., Rannik, Ü., Dal Maso, M., Kulmala, M., Vesala, T., 2003. Long-term measurements of surface fluxes above a Scots pine forest in Hyytiälä, southern Finland, 1996–2001. Boreal Environ. Res. 8 (4), 287–301.
Syed, K.H., Flanagan, L.B., Carlson, P.J., Glenn, A.J., Van Gaalen, K.E., 2006. Environmental control of net ecosystem CO_2 exchange in a treed, moderately rich fen in northern Alberta. Agric. For. Meteorol. 140 (1–4), 97–114.

Tedeschi, V., Rey, A., Manca, G., Valentini, R., Jarvis, P.G., Borghetti, M., 2006. Soil respiration in a Mediterranean oak forest at different developmental stages after coppicing. Global Change Biol. 12 (1), 110–121.

Thomas, C.K., Law, B.E., Irvine, J., Martin, J.G., Pettijohn, J.C., Davis, K.J., 2009. Seasonal hydrology explains interannual and seasonal variation in carbon and water exchange in a semiarid mature ponderosa pine forest in central Oregon. J. Geophys. Res. 114 (G04006), doi:10.1029/2009JG001010.

Tognetti, R., Longobucco, A., Miglietta, F., Raschi, A., 1999. Water relations, stomatal response and transpiration of Quercus pubescens trees during summer in a Mediterranean carbon dioxide spring. Tree Physiol. 19 (4–5), 261–270.

Tolk, J.A., Howell, T.A., Evett, S.R., 2006. Nighttime evapotranspiration from alfalfa and cotton in a semiarid climate. Agron. J. 98 (3), 730–736.

Trenberth, K.E., Smith, L., Qian, T.T., Dai, A.G., Fasullo, J., 2007. Estimates of the global water budget and its annual cycle using observational and model data. J. Hydrometeorol. 8 (4), 758–769.

Verma, S.B., Dobermann, A., Cassman, K.G., Walters, D.T., Knops, J.M., Arkebauer, T.J., Suyker, A.E., Burba, G.G., Amos, B., Yang, H.S., Ginting, D., Hubbard, K.G., Gitelson, A.A., Walter-Shea, E.A., 2005. Annual carbon dioxide exchange in irrigated and rainfed maize-based agroecosystems. Agric. For. Meteorol. 131 (1-2), 77–96.

Verma, S.B., Kim, J., Clement, R.J., 1992. Momentum, water-vapor, and carbon-dioxide exchange at a centrally located Prairie site During FIFE. J. Geophys. Res. 97 (D17), 18629–18639.

Vickers, D., Gockede, M., Law, B., 2010. Uncertainty estimates for 1-hour averaged turbulence fluxes of carbon dioxide, latent heat and sensible heat. Tellus B 62, 87–99.

Wan, Z.M., 2008. New refinements and validation of the MODIS land-surface temperature/emissivity products. Remote Sens. Environ. 112 (1), 59–74.

White, D.A., Turner, N.C., Galbraith, J.H., 2000. Leaf water relations and stomatal behavior of four allopatric Eucalyptus species planted in Mediterranean southwestern Australia. Tree Physiol. 20 (17), 1157–1165.

Wilson, K.B., Baldocchi, D.D., Aubinet, M., Berbigier, P., Bernhofer, C., Dolman, H., Falge, E., Field, C., Goldstein, A., Granier, A., Grelle, A., Halldor, T., Hollinger, D., Katul, G., Law, B.E., Lindroth, A., Meyers, T., Moncrieff, J., Monson, R., Oechel, W., Tenhunen, J., Valentini, R., Verma, S., Vesala, T., Wofsy, S., 2002. Energy partitioning between latent and sensible heat flux during the warm season at FLUXNET sites. Water Resour. Res. 38 (12), doi:10.1029/2001WR000989.

Wright, I.J., Reich, P.B., Westoby, M., Ackerly, D.D., Baruch, Z., Bongers, F., Cavender-Bares, J., Chapin, T., Cornelissen, J.H.C., Diemer, M., Flexas, J., Garnier, E., Groom, P.K., Gulias, J., Hikosaka, K., Lamont, B.B., Lee, T., Lee, W., Lusk, C., Midgley, J.J., Navas, M.L., Niinemets, U., Oleksyn, J., Osada, N., Poorter, H., Poot, P., Prior, L., Pyankov, V.I., Roumet, C., Thomas, S.C., Tjoelker, M.G., Veneklaas, E.J., Villar, R., 2004. The worldwide leaf economics spectrum. Nature 428 (6985), 821–827.